Contrasting Products in the Reactions of Cr, Mo, and W Atoms with H_2O_2: Argon Matrix Infrared Spectra and Theoretical Calculations

Xuefeng Wang and Lester Andrews*

Chemistry Department, University of Virginia, P. O. Box 400319, Charlottesville, Virginia 22904-4319

Received: May 17, 2006; In Final Form: June 14, 2006

Products in the reactions of H_2O_2 and H_2, O_2 mixtures have been observed by matrix infrared absorptions and identified through comparisons with vibrational frequencies calculated for these molecules. The chromium reactions are dominated by lower oxidation state products, whereas molybdenum and tungsten chemistry favors higher oxidation state products. For example chromium dihydroxide, $Cr(OH)_2$, molybdenum hydride oxide, H_2MoO_2, and tungsten hydride oxide, H_2WO_2, were observed in laser-ablated metal atom reactions with H_2O_2, and calculations show that these are the most stable molecules for this stoichiometry. Chromium monohydroxide, CrOH, was identified through O−H and Cr−O stretching modes, while HWO was observed by W−H and W═O stretching modes. The metal oxyhydroxides, HMO(OH), were observed for all metals. However, reactions with two H_2O_2 molecules give $OCr(OH)_2$, $MoO_2(OH)_2$, and $WO_2(OH)_2$. The relative stabilities of different structures for Cr, Mo, and W are due to different participations of occupied d orbitals. The reactivity of the cold metal atoms with H_2O_2 on annealing the solid argon matrix increases on going down the group.

Introduction

Because of different d orbital participation in σ bonding and polarization of the outermost core shells, the chemistries of chromium and tungsten are dramatically different, although the two metals are located in the same transition metal group. For example, tungsten reacts with H_2 in solid neon, giving trigonal prismatic C_{3v} hexahydride, WH_6, while only the hydride complex, $CrH_2(H_2)_2$, is obtained for the chromium case and molybdenum appears to be like tungsten.[1] In addition the reaction of tungsten with CH_4 gave three hydrides, CH_3—WH, CH_2═WH_2, and CH≡WH_3, and spectra were dominated by the most stable trihydride CH≡WH_3, and all three products were also observed for Mo, but in contrast CH_3—CrH is the most stable and the only chromium product trapped in solid argon.[2] Furthermore, WH_6 was found to be a simple model for "non-VSEPR" systems.[1,3,4] Both WF_6 and WCl_6 are stable molecules observed experimentally, while CrF_6 is calculated to be stable with respect to Cr−F dissociation.[5−10] Up to now there are no experimental data available for CrF_6 and $CrCl_6$.

Recently we have developed a new method to explore metal hydroxide molecules using laser-ablated metal reactions with H_2O_2 or $H_2 + O_2$ mixtures in low-temperature matrixes.[11−15] With this method we have the advantage of identifying most infrared active modes without overlapping of water absorptions. For example ionic hydroxides $M(OH)_2$ (M = group 2 metals), $M(OH)_2$ and $M(OH)_4$ (M = group 4 metals), and covalent hydroxides $M(OH)_2$ (M = group 11 metals and Hg) have been investigated.

We present here an extensive matrix infrared spectroscopic study of laser-ablated chromium, molybdenum, and tungsten atom reactions with H_2O_2 and $H_2 + O_2$ mixtures in solid argon. Several new metal hydroxides, oxyhydroxides, and hydride oxides are identified from matrix isolation infrared spectroscopy and theoretical vibrational frequency calculations.

* To whom correspondence should be addressed. E-mail: lsa@virginia.edu.

Experimental and Computational Methods

Laser-ablated Cr, Mo, and W atom reactions with small molecules in excess argon at 10 K have been described in our previous papers.[1,16,17] The Nd:YAG laser fundamental (1064 nm, 10 Hz repetition rate with 10 ns pulse width) was focused onto a rotating metal target (Johnson Matthey), which gives a bright plume spreading uniformly to the 10 K CsI window. The chromium, molybdenum, and tungsten targets were polished to remove the oxide coating and immediately placed in the vacuum chamber. The laser energy was varied about 10−20 mJ/pulse. FTIR spectra were recorded at 0.5 cm^{-1} resolution on Nicolet 750 with 0.1 cm^{-1} accuracy using an MCTB detector. Matrix samples were annealed at different temperatures, and selected samples were subjected to irradiation using a medium-pressure mercury arc lamp (Philips, 175 W) with the globe removed.

Urea hydrogen peroxide (UHP; Aldrich, 98%) was used to provide pure H_2O_2, which was put in a glass tube at room temperature and pumped about 1 h to remove H_2O. Argon gas was passed over UHP, which released H_2O_2 to mix with excess argon (approximately 0.1−0.2% concentration) on deposition. Deuterated urea−D_2O_2 was prepared as described by Pettersson et al.[18,19] Additional supporting experiments were done with samples of H_2, D_2, or HD, and O_2, $^{18}O_2$, or $^{16,18}O_2$ mixtures.

Complementary density functional theory (DFT) calculations were performed using the Gaussian 98 program,[20] B3LYP calculations, the 6-311++G(3df,3pd) basis set for hydrogen and oxygen atoms, and SDD pseudopotential and basis for chromium, molybdenum, and tungsten. All of the geometrical parameters were fully optimized, and the harmonic vibrational frequencies were obtained analytically at the optimized structures.

Results

Infrared spectra of products formed in the reactions of laser-ablated chromium, molybdenum, and tungsten atoms with H_2O_2 or H_2 and O_2 mixtures in excess argon during condensation at

10.1021/jp063024m CCC: $33.50
Published on Web 07/22/2006

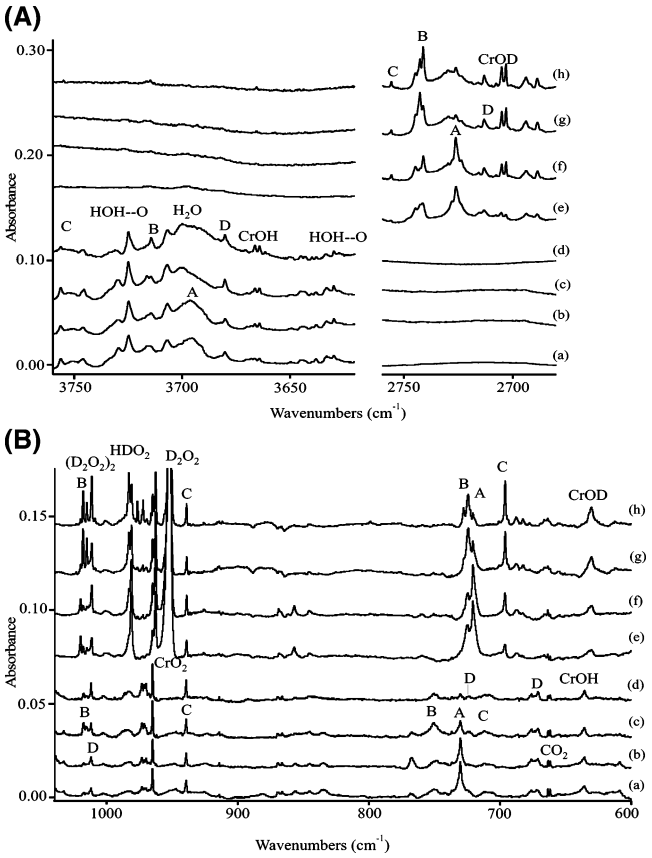

Figure 1. Infrared spectra for chromium atom and H_2O_2 reaction products in solid argon at 10 K. Cr + H_2O_2 deposition (a) for 60 min, (b) after annealing to 20 K, (c) after 240−380 nm irradiation, and (d) after >220 nm irradiation. Cr + D_2O_2 deposition (e) for 60 min, (f) after >290 nm irradiation, (g) after 240−380 nm irradiation, and (h) after >220 nm irradiation.

10 K will be presented in turn. Density functional calculations were performed to support the identifications of new reaction products. Common species, such as O_3, O_4^-, HO_2, and Ar_nH^+, have been identified in previous papers.[21−24]

Cr + H_2O_2. Infrared spectra of laser-ablated chromium atoms co-deposited with H_2O_2 in excess argon at 10 K, with annealing and irradiation afterward (Figure 1), gave six groups of product bands. Group A bands at 3696.4 cm^{-1} beside water and at 730.3 cm^{-1} generated on deposition decreased 30% on annealing, further decreased 70% on 240−380 nm irradiation, and totally bleached on full-arc irradiation. With D_2O_2 these bands shift to 2726.1 and 720.6 cm^{-1}, respectively, with similar annealing and irradiation behaviors as observed with H_2O_2. Group B bands at 3716.4, 1752.9, and 749.0 cm^{-1} formed weakly on deposition increased slightly on annealing to 20 K, and increased substantially on 240−380 nm irradiation, which is at the expense of group A bands. The deuterium counterparts of these bands were found at 2742.6, 1298.3, and 728.6 cm^{-1}. Group C bands at 3745.8, 939.6, and 712.0 cm^{-1} appeared on deposition, increased 30% on full-arc irradiation and decreased slightly on further annealing. With D_2O_2 these bands shift to 2755.7, 939.3, and 696.2 cm^{-1}, respectively. Group D bands appeared at 3680.2 and 1002.9 cm^{-1}, increased slightly on irradiation cycles, and shifted to 2713.1 and 1001.4 cm^{-1} with D_2O_2. Bands in group E were observed at 3645.1, 724.6, and 670.9 cm^{-1}. The final 3666.2, 635.0, cm^{-1} group (CrOH) increased markedly on irradiation and shifted to 2705.0, 630.2 cm^{-1} with D_2O_2. The bands labeled HOH—O are due to a H_2O_2 photolysis product

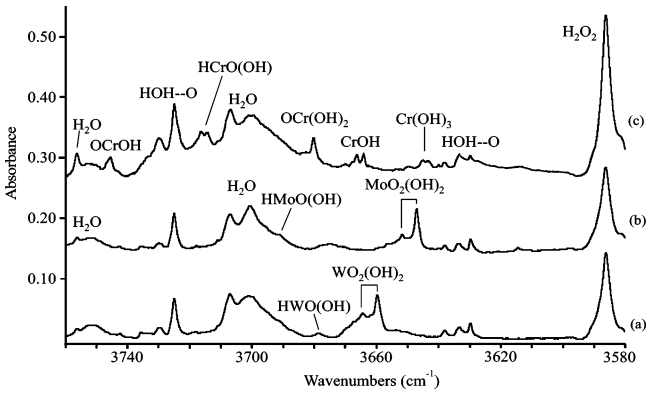

Figure 2. Infrared spectra for Cr, Mo, and W atom reaction products with H_2O_2 in solid argon at 10 K all after 60 min co-deposition and full-arc irradiation (>220 nm): (a) Cr + H_2O_2; (b) Mo + H_2O_2; (c) W + H_2O_2.

TABLE 1: Infrared Absorptions (cm^{-1}) Observed for Products of the Reactions of Cr Atoms with H_2O_2 or H_2 + O_2 Molecules

H_2O_2/ H_2+O_2	D_2O_2/ D_2+O_2	$H_2+{}^{18}O_2$	$D_2+{}^{18}O_2$	identification
3746.1/3745.5	2755.7/−	3733.6	2745.0	OCr(OH) (C)
3714.6/3714.6	2742.6/2741.2	3702.9	2733.8	HCrO(OH) (B)
3696.4/3695.1	2726.1/2725.1	3683.4	2715.6	$Cr(OH)_2$ (A)
3680.2/3680.2	2712.1	3670.6	2696.9	$Cr(OH)_3$
3666.2	2705.0			CrOH
3664.2	2703.1			CrOH
1752.9/1753.1	1267.4/1267.6	1753.1	1267.4	HCrO(OH) (B)
1012.2/1012.4	1011.8/1011.8	971.5	970.6	HCrO(OH) (B)
1002.9/1002	1001.4/1001.8	960.6	959.9	$OCr(OH)_2$
939.6/939.9	939.3/939.5	903.2	902.6	OCr(OH) (C)
749.0/750	724.3/−	725.8	704.1	HCrO(OH) (B)
730.3/730.5	720.6/720	709.2	698.7	$Cr(OH)_2$ (A)
724.6	718.4			$Cr(OH)_3$
712.0/−	696.2/−	686.8	676.4	OCr(OH) (C)
670.9	505.7			$Cr(OH)_3$
635.6	630.2			CrOH

described previously.[12,14,19] Figure 2 contrasts spectra in the upper region for Cr, Mo, and W reactions with H_2O_2.

Weak absorptions of CrO (846.3 cm^{-1}) and CrO_2 (965.3 and 914.4 cm^{-1})[25] arises partly from the metal oxide on the target surface and partly from decomposition of chromium hydroxides.

Cr + H_2 + O_2. This experiment is basically the same as those of early investigations with each reagent separately,[1,25] but additional new product bands were observed using the reagent mixture. The B, C, D, and E product absorptions were stronger with this reagent mixture than with H_2O_2. In contrast group A bands were produced on >290 nm irradiation and decreased by shorter wavelength irradiation in favor of the group B absorptions. Complementary experiments were done with ^{18}O and deuterium substitution, and the absorptions are listed in Table 1. The binary chromium oxides and hydrides were also observed.[1,25]

Mo + H_2O_2. Experiments were done with Mo and H_2O_2 or D_2O_2, and new product bands were observed in the O−H stretching region at 3690.8 and 3647.2 cm^{-1}, in the Mo−H stretching region at 1864.0, 1861.0, and 1781.5 cm^{-1}, in the Mo═O stretching region at 985.0 and 979.3 cm^{-1}, and in the Mo−O stretching region at 732.1 and 712.6 cm^{-1}. Molybdenum oxide bands were also observed.[26] Figure 3 shows a spectrum with Mo and H_2O_2, and Table 2 lists the observed frequencies: the product yield was not as good with the H_2 and O_2 reagent mixture.

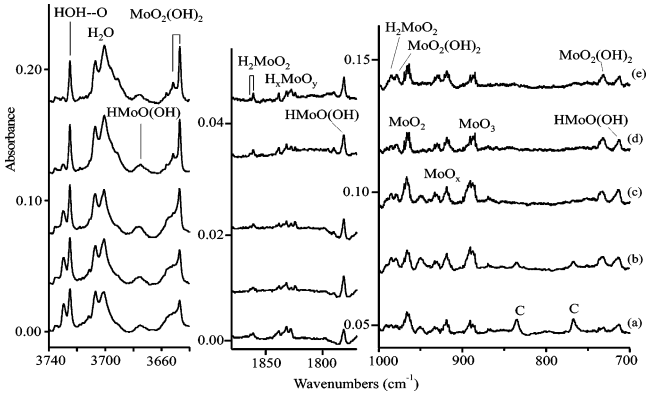

Figure 3. Infrared spectra for molybdenum atom and H_2O_2 reaction products in solid argon at 10 K. Mo + H_2O_2 deposition (a) for 60 min, (b) after 240−380 nm irradiation, (c) after >220 nm irradiation, (d) after annealing to 20 K, and (e) after annealing to 26 K.

TABLE 2: Infrared Absorptions (cm^{-1}) Observed for Products of the Reactions of Mo Atoms with H_2O_2 or $H_2 + O_2$ Molecules

H_2O_2/ $H_2 + O_2$	D_2O_2/ $D_2 + O_2$	$H_2+{}^{18}O_2$	$D_2+{}^{18}O_2$	identification
3690.8	2710.1			HMoO(OH)
3651.7/3651.9[a]	2691.2/2693.1[a]	3640.4	2676.5	$MoO_2(OH)_2$
3647.2/3647.4[a]	2688.6/2688.8[a]	3636.1	2672.5	$MoO_2(OH)_2$
1864.0				H_2MoO_2
1861.0	1337.8			H_2MoO_2
1781.5	1280.1			HMoO(OH)
985.0	985	924	924	H_2MoO_2
979.3	—[b]			$MoO_2(OH)_2$
732.1	703.2			$MoO_2(OH)_2$
712.6	693.7			HMoO(OH)

[a] In H_2O_2 + D_2O_2 experiment two median bands at 3649.4 and 2690.9 cm^{-1} were found. [b] Covered by absorption of D_2O_2 dimer.

W + H_2O_2. Figure 4 illustrates spectra of the products of laser-ablated W atom reactions with H_2O_2 in excess argon. New absorptions were observed at 3691.2 cm^{-1} (weak) and 3664.4, 3661.9, 3659.7 cm^{-1} (strong) in the O−H stretching region, from 1958.7 to 1790.2 cm^{-1} in the W−H stretching region, at 1010.1, 1003.6 cm^{-1} (weak), 984.2, 969.2, 965.7 cm^{-1} (strong), 953.0, 948.0 cm^{-1} (weak) in the W═O stretching region, and at 734.9, 726.3, 641.5, and 614.9 cm^{-1} in the W−O stretching region on deposition. These bands increased slightly on UV irradiation. Tungsten oxide bands were also observed in both H_2O_2 and D_2O_2 experiments.[26]

W + H_2 + O_2. Similar absorptions as mentioned above were observed in three W + H_2 + O_2 experiments, but the 3659.7, 1003.3, and 966.0 cm^{-1} bands increased markedly on UV irradiation. For isotopic reagent substitution several experiments were done with $^{16}O_2$ + D_2 or HD, and the substituted absorptions are listed in Table 3. Spectra from reactions with different oxygen isotopic precursors are illustrated in Figure 5. The major photolysis product reveals new absorptions with the mixed isotopic precursor. Absorptions of WH_x ($x = 1-6$) and tungsten oxides were observed that have been identified in our earlier investigatons.[1,26]

Calculations. Different oxidation state products (M(II), M(IV), and M(VI)) for Cr, Mo, and W with H_2O_2 must be considered, and calculated energies and geometries for several of these products are summarized in Figures 6 and 7. The Cr atom reaction with H_2O_2 is predicted to form $Cr(OH)_2$ with C_2 symmetry (^{5}A) as the lowest energy product, and higher energy products include HCrO(OH) with C_s symmetry (^{3}A″) [computed 25 kcal/mol higher in energy] and H_2CrO_2 [67 kcal/mol higher

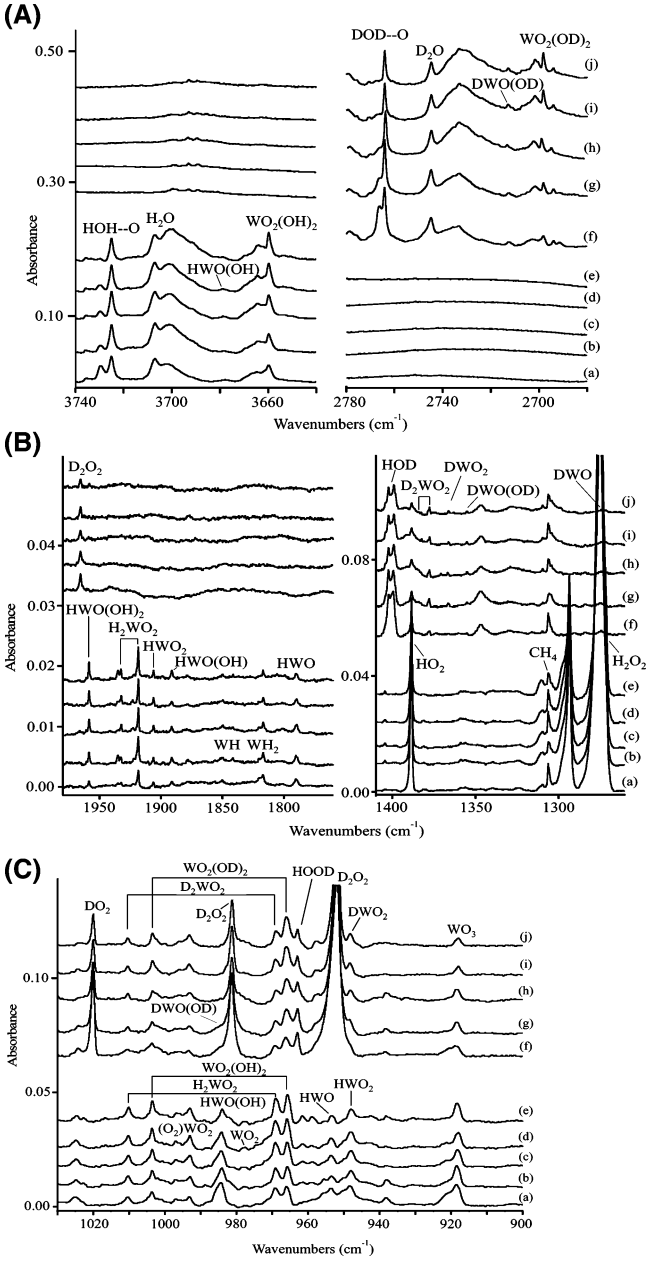

Figure 4. Infrared spectra for tungsten atom reaction products with H_2O_2 in solid argon at 10 K. (a) W + H_2O_2 deposition for 60 min, (b) after annealing to 20 K, (c) after 240−380 nm irradiation, and (d) after > 220 nm irradiation, (e) after annealing to 26 K. (f) W + D_2O_2 deposition for 60 min, (g) after annealing to 20 K, (h) after annealing to 32 K, (i) after > 220 nm irradiation, and (j) after annealing to 32 K.

in energy than $Cr(OH)_2$]. The higher hydroxides $Cr(OH)_3$ and $Cr(OH)_4$ were also calculated.

For tungsten the reverse case is obtained: H_2WO_2 (W(VI)) is calculated lowest in energy, while HWO(OH) is 17 kcal/mol higher, the $(H_2)WO_2$ complex is 43 kcal/mol higher, and $W(OH)_2$ lies highest with 54 kcal/mol in energy. A new stable molecule $WO_2(OH)_2$ has also been calculated, and the structure is shown in Figure 6.

It is interesting to note that, for molybdenum, H_2MoO_2 and HMo(OH) are predicted to be energetically equivalent isomers, while $Mo(OH)_2$ lies 20 kcal/mol higher and the $(H_2)MoO_2$ complex is the highest energy at 26 kcal/mol.

The M(III) species, OMOH M = Cr, Mo, W, were also calculated, and all three gave C_s symmetry with ^{4}A″ ground states. Similarly the chromium monohydroxide, CrOH (^{6}A′) is 35 kcal/

TABLE 3: Infrared Absorptions (cm^{-1}) Observed for Products of the Reactions of W Atoms with H_2O_2 or $H_2 + O_2$ Molecules

H_2O_2/ $H_2 + O_2$	D_2O_2/ $D_2 + O_2$	$H_2 + {}^{18}O_2$	$HD + O_2$	identification
3678.6	2712.6			HWO(OH)
3664.4	2701.5/2701.7			$WO_2(OH)_2$
3661.9	2700.4			$HWO_2(OH)$
3659.7/3659.7	2698.1/2698.3	3648.7	3659.8, 3662.5 2698.2, 2700.6	$WO_2(OH)_2$
1958.7	—[a]			$HWO_2(OH)$
1932.4	1382.5	1932.5	1924.8	H_2WO_2
1918.5	1377.6	1918.5	1381.2	H_2WO_2
1906.1	1366.4	1906.1		HWO_2
1891.5	1355.2			HWO(OH)
1790.2	1283.9			HWO
1010.1/1010.3	1010.1/1010.6			H_2WO_2
1003.6	1003.6	950.3	1003.6	$WO_2(OH)_2$
984.2	—[a]	935.7		HWO(OH)
969.2	969.0	918.3	969.2	H_2WO_2
965.7	965.7	916.9	966.0	$WO_2(OH)_2$
953.5	—[a]			HWO
948.0	948.0	896.3	948.1	HWO_2
726.3	699.3			$WO_2(OH)_2$
641.5				$WO_2(OH)_2$
614.9				$WO_2(OH)_2$

[a] Covered by absorption of D_2O_2 system.

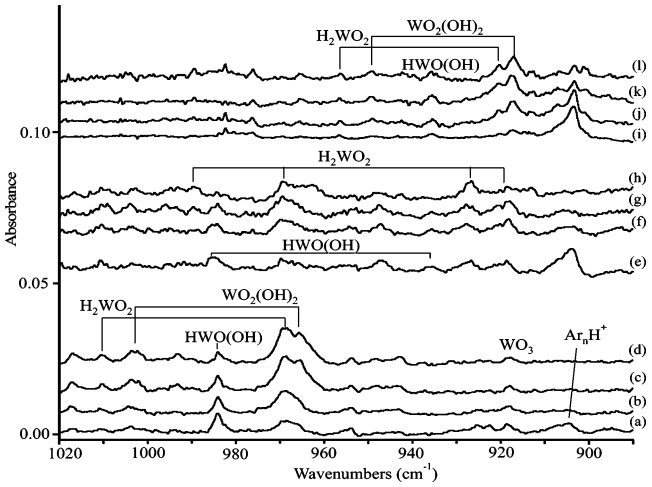

Figure 5. Infrared spectra for tungsten atom and hydrogen and isotopic oxygen reaction products in solid argon at 10 K. W + H_2 + $^{16}O_2$ deposition (a) for 60 min, (b) after 240−380 nm irradiation, (c) after >220 nm irradiation, and (d) after annealing to 22 K. W + H_2 + $^{16}O_2$ + $^{16}O^{18}O$ + $^{18}O_2$ deposition (e) for 60 min, (f) after 240−380 nm irradiation, (g) after >220 nm irradiation, and (h) after annealing to 20 K. W + H_2 + $^{18}O_2$ deposition (i) for 60 min, (j) after 240−380 nm irradiation, (k) after > 220 nm irradiation, and (l) after annealing to 20 K.

mol lower than HCrO ($^4A'$) in energy, while HWO ($^4A''$) is located 25 kcal/mol lower in energy than WOH ($^6A'$).

Discussion

The new chromium, molybdenum, and tungsten hydroxide, oxyhydroxide, and hydride oxide molecules will be identified through different reaction mixtures, photochemical properties, isotopic substitution, and comparison with theoretical frequency calculations.

CrOH. A doublet at 3666.2 and 3664.2 cm^{-1} [due to matrix site splitting] in Cr + H_2O_2 experiments appeared on deposition and increased slightly on annealing and irradiation. A weak band at 635.6 cm^{-1} tracks with the upper bands on irradiation and annealing. With D_2O_2 the upper bands shift to 2705.0 and 2703.1 cm^{-1} (H/D = 1.3553) and the lower band shifts to 630.2 cm^{-1}

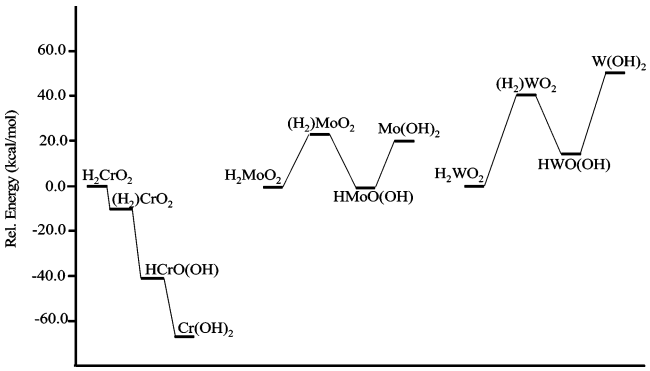

Figure 6. Relative energies of group 6 hydroxide molecules computed at the B3LYP level of theory using the 6-311++G(3df,3pd) basis for H and O, and SDD pseudopotentials for Cr, Mo, and W.

(H/D = 1.0086). With the H_2O_2 + D_2O_2 mixture all bands from separate H_2O_2 and D_2O_2 experiments were observed. Unfortunately these bands were not observed in H_2 + O_2 and H_2 + D_2 experiments, so no ^{18}O data for these bands could be obtained. Apparently this species is generated directly from the Cr reaction with H_2O_2, and CrOH is an appropriate absorber for these bands.

Our DFT calculation supports this assignment. The O−H and Cr−O stretching modes are predicted at 3848.5 and 638.6 cm^{-1}, respectively. The O−H stretching mode is overestimated by 5.0%, which is in good agreement with other chromium hydroxide calculations. The Cr−O stretching mode is only overestimated by 3 cm^{-1}, which is in line with chromium oxide work.[25]

A laser-ablated Cr atom with high kinetic energy can break the O−O bond of H_2O_2 giving CrOH, which is trapped in the cold argon matrix.

$$Cr + H_2O_2 \rightarrow Cr(OH) + OH \quad (1)$$

$Cr(OH)_2$. A strong new infrared absorption at 730.3 cm^{-1} in the Cr−O stretching region tracks the 3696.4 cm^{-1} band beside water in the O−H stretching region from the Cr + H_2O_2 reaction, which is generated on deposition, decreased by 10% on annealing to 20 K, further decreased by 70% on 240−380 nm irradiation, and destroyed by full-arc irradiation. With the D_2O_2 reagent, the Cr−O band shifts to 720.6 cm^{-1} and the O−H band to 2726.1 cm^{-1}, respectively. The red shifts of the Cr−O stretching mode with D-substitution indicate this mode coupled by H atom and O−H stretching mode gives a 1.3559 H/D ratio, which is typical for transition metal hydroxides we discussed in our earlier papers.[12−15] In addition the Cr−O stretching frequencies of CrO (846.3 cm^{-1}) and CrO_2 (965.3, 914.4 cm^{-1}) were also observed.[25] The new 730.3 cm^{-1} Cr−O stretching mode is substantially lower than the same mode for oxides CrO and CrO_2, which suggests very strong H coupling for this mode. Complementary experiments using Cr atom reactions with the H_2 + O_2 mixture gave very weak bands centered at 730.5 and 3695.1 cm^{-1}, which increased on 290−700 nm irradiation, but decreased on 240−380 nm and disappeared on full-arc irradiation. These bands shift to 709.2 and 3683.4 cm^{-1} with Cr + H_2 + $^{18}O_2$. The isotopic frequency patterns with $^{16}O_2$ + $^{16,18}O_2$ + $^{18}O_2$ (1:2:1) show a triplet pattern with a 720.1 cm^{-1} intermediate component, suggesting that two equivalent oxygen atoms are involved. The two upper modes give a doublet at 3695 and 3683 cm^{-1}, indicating very little or no coupling between two O−H groups. Therefore the $Cr(OH)_2$ molecule is proposed. Note that the frequencies differ up to 1 cm^{-1} for products produced by the stoichiometrically equivalent but different photochemical

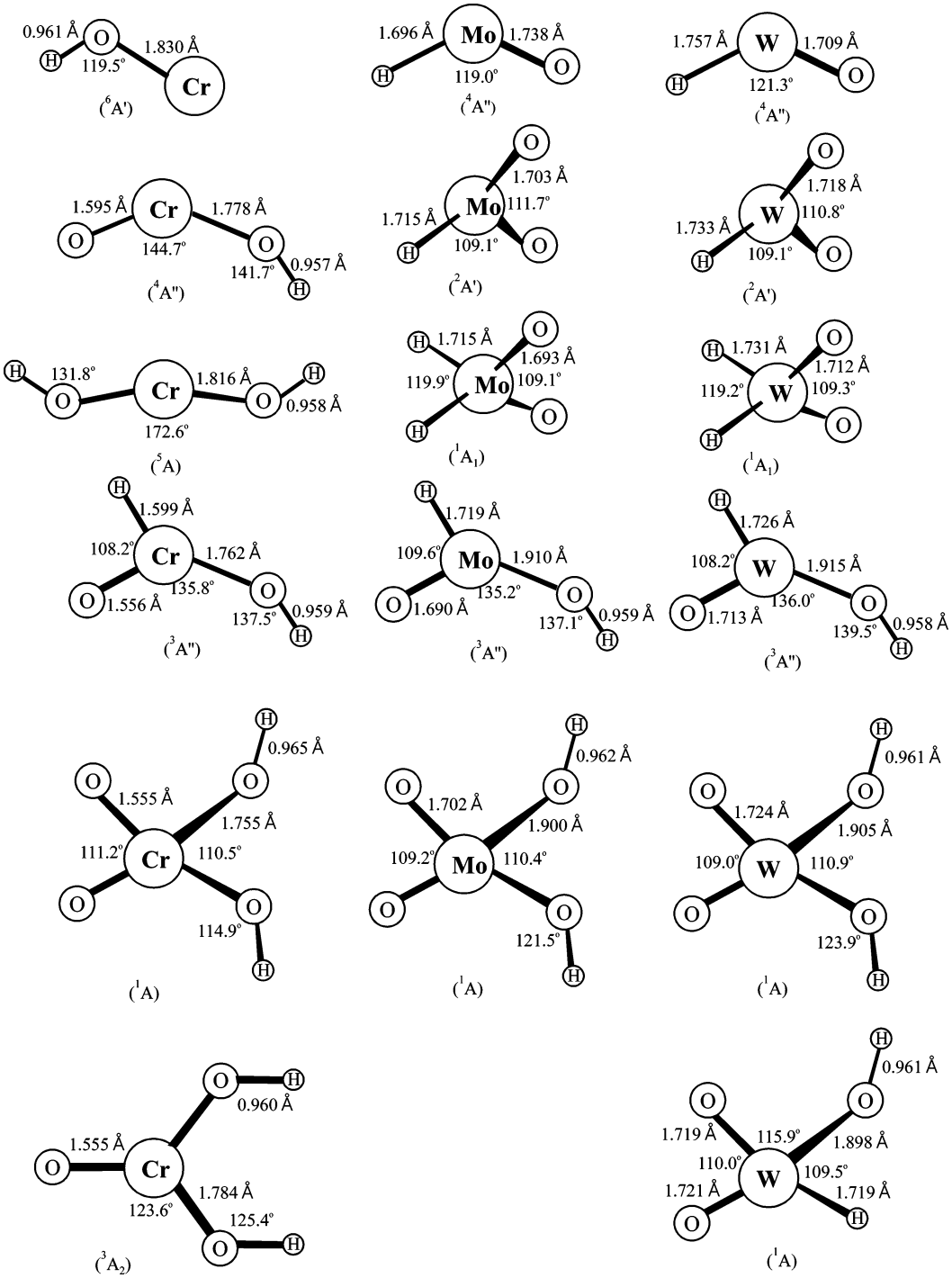

Figure 7. Structures of the group 6 hydroxide molecules computed at the B3LYP level of theory using the 6-311++G(3df,3pd) basis for H and O, and SDD pseudopotentials for Cr, Mo, and W.

reactions with H_2O_2 and with H_2 and O_2: both sets of frequencies are given in Table 1.

The identification of $Cr(OH)_2$ is confirmed by B3LYP calculations (Table 4). The Cr−O and O−H stretching modes are predicted at 3893.9 and 743.3 cm^{-1} overestimated by 5.3 and 1.8%, respectively, which are the typical for transition metal hydroxides.[11−15] The predicted H/D and 16/18 isotopic ratios also match experimental values very well.

Laser-ablated energetic Cr atoms react with H_2O_2 to give $Cr(OH)_2$ that is relaxed in the cold argon matrix (reaction 2): without this relaxation of reaction exothermicity by the matrix, the dihydroxide may decompose to CrOH, the product of reaction 1. We observe no evidence for a $(Cr)(H_2O_2)$ complex that might be the precursor for reaction 2. The Cr atom reaction with $O_2 + H_2$ proceeds first through CrO_2, which we believe inserts into H_2 upon irradiation most likely involving a (H_2)-CrO_2 complex,[27] to give $Cr(OH)_2$ (reaction 3). Similar reactions have been proposed for other transition metal atoms.[11−15]

$$Cr + H_2O_2 \rightarrow Cr(OH)_2 \quad (2)$$

$$Cr + O_2 + H_2 \rightarrow (H_2)CrO_2 \rightarrow Cr(OH)_2 \quad (3)$$

HCrO(OH). The A group of bands at 1753.1 cm^{-1} (Cr−H stretching), 1012.2 cm^{-1} (Cr═O stretching), 749.0 cm^{-1} (Cr−O) stretching), and 3714.6 cm^{-1} (O−H stretching) track together:

TABLE 4: Calculated Frequencies (cm^{-1}) of $Cr(OH)_2$ at the B3LYP Level of Theory and Comparison with Experimental Results

$Cr(OH)_2$		$Cr(OD)_2$		$Cr(^{18}OH)_2$		$Cr(^{18}OD)_2$	
calcd	obsd	calcd	obsd	calcd	obsd	calcd	obsd
3895.6(a,24)		2837.1(14)		3882.7(23)		2818.9(14)	
3893.9(b,153)	3696.4	2835.4(112)	2726.1	3881.1(146)	3683.4	2817.4(104)	2715.6
743.3(b,271)	730.3	732.4(307)	720.6	719.8(243)	709.2	709.5(282)	698.7
617.9(a,0)		600.8(3)		587.6(2)		568.8(2)	
498.4(a,0)		380.6(56)		495.5(0)		375.7(54)	
496.8(a,89)		370.0(0)		490.2(84)		366.2(0)	
452.1(b,174)		336.1(83)		448.9(177)		332.8(83)	
161.7(a,2)		150.9(1)		157.2(2)		147.7(1)	
78.1*i*(b,1)		71.1*i*(7)		77.8*i*(1)		68.7*i*(5)	

TABLE 5: Calculated Frequencies (cm^{-1}) of HCrO(OH) at the B3LYP Level of Theory and Comparison with Experimental Results

HCrO(OH)		DCrO(OD)		$HCr^{18}O(^{18}OH)$		$DCr^{18}O(^{18}OD)$	
calcd	obsd	calcd	obsd	calcd	obsd	calcd	obsd
3899.9(a205)	3714.6	2841.2(137)	2741.2	3886.9(198)	3702.9	2822.8(129)	2733.8
1869.6(a,132)	1752.9	1336.8(75)	1267.4	1869.6(132)	1753.1	133.6(75)	1267.4
1075.5(a,224)	1012.2	1074.1(218)	1011.8	1030.9(215)	971.5	1029.2(209)	970.6
763.7(a,110)	749.0	737.1(128)	724.3	735.9(91)	725.8	707.6(112)	704.1
638.0(a,17)		468.6(16)		633.9(16)		465.5(14)	
510.0(a,110)		408.8(40)		501.4(113)		400.1(43)	
399.0(a,165)		324.7(101)		393.8(163)		318.2(99)	
213.0(a,16)		193.6(16)		206.1(14)		188.6(15)	
149.8(a,11)		112.2(4)		149.4(11)		111.9(4)	

TABLE 6: Observed and Calculated Frequencies (cm^{-1}) for OM(OH) (M = Cr,W), CrOH, and HWO

OCr(OH) ^{4}A		OCr(OD)		OW(OH) ^{4}A	OW(OD)
calcd	obsd	calcd	obsd	calcd	calcd
3915.1(178)	3746.1	2852.8(123)	2755.7	3912.0(181)	2857.7(125)
981.0(225)	939.6	980.6(227)	939.3	981.2(164)	981.2(164)
726.4(82)	712.0	704.0(102)	696.2	686.1(98)	659.5(139)
522.2(134)		415.5(68)		519.5(155)	409.2(67)
415.9(89)		325.1(56)		443.9(92)	344.8(51)
152.7(18)		141.9(17)		137.5(7)	129.5(7)

CrOH ^{6}A		CrOD		HWO ^{4}A		DWO	
calcd	obsd	calcd	obsd	calcd	obsd	calcd	obsd
3848.5(62)	3666.2	2801.2(44)	2705.0	1858.0(172)	1790.2	1319.1(82)	1283.9
654.1(25)		472.1(50)		986.6(149)	953.5	985.5(148)	–
638.6(222)	635.6	643.2(159)	630.2	540.0(23)		397.0(11)	

they were observed weakly on deposition, increased slightly on annealing to 20 K, and increased 2-fold on 240−380 nm irradiation. The increase of these bands on annealing and on irradiation is most likely at the expense of $Cr(OH)_2$. Except for the Cr−O stretching mode, all other bands were observed in experiments of Zhou et al. for Cr with $H_2 + O_2$ and CrO_3 with H_2 in solid argon.[27] At this point our results are in agreement, and the HCrO(OH) assignment is accepted. With D_2O_2 the Cr−H mode shifts to 1298.3 cm^{-1} (H/D = 1.3503), the Cr═O mode shifts to 1011.8 cm^{-1} band (very slightly coupled with H), the Cr−O stretching mode shifts to 724.3 cm^{-1} (coupled with H, H/D = 1.0341), and the O−H stretching mode shifts to 2742.6 cm^{-1} (H/D = 1.3419). Complementary experiments were done with $Cr + H_2 + O_2$ and isotopic substitutions, which are in good agreement with Zhou et al. In addition, the theoretical calculations strongly support this assignment (Table 5).

The $Cr(OH)_2$ molecule is isomerized to HCrO(OH) through 240−380 nm irradiation although the reaction is endothermic by 25 kcal/mol (reaction 4a). In fact HCrO(OH) is observed on deposition, indicating photoisomerization also occurs from the laser-generated plume. The slight growth of HCrO(OH) on annealing further suggests that reaction 2 proceeds with cold Cr atoms, but its exothermicity is sufficient to drive the rearrangement reaction 4b.

$$Cr(OH)_2 + 240-380\ nm \rightarrow HCrO(OH) \quad (4a)$$

$$Cr + H_2O_2 \rightarrow Cr(OH)_2 \rightarrow HCrO(OH) \quad (4b)$$

OCrOH. A sharp band at 939.6 cm^{-1} (Cr═O stretching) tracks the 712.0 cm^{-1} band (Cr−O stretching) and 3746.1 cm^{-1} band (O−H stretching), which appeared in the H_2O_2 experiment on deposition, increased on full-arc irradiation, and decreased on further annealing. The same bands were observed in Cr with $H_2 + O_2$. With D_2O_2 the OD stretching mode appeared at 2755.7 cm^{-1}, giving a 1.3594 H/D ratio, while Cr═O stretching mode shifts down only 0.3 cm^{-1}, suggesting very little coupling with H, but the Cr−O stretching mode exhibits a 24.4 cm^{-1} red shift and demonstrates a large H coupling. Our B3LYP calculation reproduced frequencies very well, as compared in Table 6.

OCr(OH)$_2$. The sharp band at 3680.2 cm^{-1} (O−H stretching mode) observed in $Cr + H_2O_2$ experiments increased slightly on full-arc irradiation and tracked with a weak band at 1002.9 cm^{-1} in the Cr═O stretching region. With $Cr + D_2O_2$ the O−D stretching mode shifted to 2713.1 cm^{-1} (H/D = 1.3565) and the Cr═O mode shifted only slightly to 1001.4 cm^{-1}. As will be described later (see Figure 2), a major product with the heavier metals is $MO_2(OH)_2$, and this product was also computed for the Cr reagent, but the diagnostic O−H stretching mode

TABLE 7: Observed and Calculated Frequencies (cm^{-1}) for $OCr(OH)_2$ (C_{2v}), $MoO_2(OH)_2$ (C_2), and $WO_2(OH)_2$ (C_2)

$OCr(OH)_2$ $^3A_2$		$OCr(O\ D)_2$		$MoO_2(\ OH)_2$ ^1A		$MoO_2(OD)_2$		$WO_2(OH)_2$ ^1A		$WO_2(OD)_2$	
calcd	obsd	calcd	obsd	calcd	obsd	calcd	obsd	calcd	obsd	calcd	obsd
3878.6(3)		2824.6(3)		3848.1((57)	3651.7	2802.3(38)	2691.2	3866.8(51)	3664.4	2816.3(35)	2701.5
3874.3(333)	3680.2	2820.4(219)	2713.1	3844.3(329)	3647.0	2798.6(202)	2688.6	3863.1(361)	3659.7	2812.7(222)	2698.1
1071.7(215)	1002.9	1071.6(212)	1001.4	1014.7(93)		1014.7(93)		1012.1(69)		1012.0(69)	
761.2(171)		729.3(264)		1000.9(234)	979.3	999.8(228)	979.3	979.1(214)	965.7	978.5(208)	965.7
689.0(66)		682.8(82)		737.3(54)	732.1	703.9(199)	703.2	730.3(46)		697.9(96)	
626.8(119)		468.9(52)		716.0(12)		693.8(100)		722.8(20)		692.6(163)	
574.5(157)		461.0(38)		668.0(174)		510.6(43)		644.3(184)		496.4(57)	
266.7(145)		255.9(99)		649.1(251)		509.9(62)		625.6(230)		494.1(67)	
215.2(41)		201.9(39)		360.0(41)		345.1(13)		359.6(49)		341.9(18)	
210.3(4)		196.8(4)		319.0(84)		279.8(35)		307.2(104)		268.6(45)	
145.3(0)		109.8(0)		283.1(26)		247.7(2)		276.9(8)		249.5(1)	
103.0(92)*i*		77.3(49)*i*		266.5(4)		232.9(2)		258.4(6)		226.0(4)	
				233.6(23)		220.3(21)		227.7(57)		214.9(18)	
				226.1(4 0)		212.3(3 7)		226.5(2 3)		203.8(39)	
				206.7(1 0)		172.7(3 4)		208.4(2)		174.7(34)	

TABLE 8: Calculated Frequencies (cm^{-1}) of H_2MoO_2 and HMoO(OH) at the B3LYP Level of Theory and Comparison with Experimental Results

H_2MoO_2		D_2MoO_2		HMoO(OH)		DMoO(OD)	
calcd	obsd	calcd	obsd	calcd	obsd	calcd	obsd
1944.5(a_1,106)	1864.0	1384.2(80)		3894.7(a,193)	3690.8	2837.3(130)	2710.1
1939.3(b_1,152)	1861.0	1379.2(55)	1337.8	1878.6(a,172)	1781.5	1336.6(90)	1280.1
1035.7(a_1,73)		1035.1(68)		1013.8(a,207)		1012.5(19)	
1014.4(b_2,204)	985.0	1009.9(197)	985.0	715.0(a,119)	712.6	676.0(149)	693.7
754.2(a_1,63)		536.9(34)		644.6(a,12)		477.3(12)	
663.0(a_2,0)		484.4(0)		526.0(a,122)		416.0(44)	
642.8(b_2,4)		466.3(4)		405.8(a,122)		319.9(71)	
469.4(b_1,2)		365.6(3)		199.2(a,11)		185.0(11)	
346.4(a_1,2)		346.1(2)		158.7(a,15)		119.7(6)	

was predicted much lower near 3600 cm^{-1} after scaling. Hence we reasoned that the intermediate oxidation state product might be appropriate for Cr, and the subject molecule was computed. The diagnostic O−H stretching mode is predicted 20 cm^{-1} below that for $Cr(OH)_2$ and the Cr═O stretching mode is computed 4 cm^{-1} below that for HCrO(OH) (Table 7). The agreement with experimental values is good enough to support this identification of the Cr(IV) oxide dihydroxide.

$Cr(OH)_3$. The weak 3645.1, 724.6, and 670.9 cm^{-1} absorptions remain to be identified. Our B3LYP calculation for $Cr(OH)_3$ gives a strong degenerate O−H stretching mode 41 cm^{-1} below the O−H stretching modes of $Cr(OH)_2$, whereas this mode for $Cr(OH)_4$ is predicted 80 cm^{-1} lower. So assignment of $Cr(OH)_3$ is proposed for the 3645.1 cm^{-1} band 51 cm^{-1} below the $Cr(OH)_2$ band. A Cr−O stretching mode is predicted at 742.7 cm^{-1} that is very close to the same mode for $Cr(OH)_2$, so the 724.6 cm^{-1} band is assigned accordingly. The associated 670.9 cm^{-1} band follows for the strongest Cr−O−H bending mode.

We have no evidence for the tetrahydroxide of chromium, and we propose that this molecule is less stable than the heavier group 6 analogues. Accordingly, we suggest that $Cr(OH)_4$ formed in the reaction with another H_2O_2 molecule eliminates H_2O to give $OCr(OH)_2$. The trihydroxides have been observed with group 3 metals,[14] the elimination of water gives rise to the OMOH molecules, and this is likely to occur with Cr as well as Mn and Fe.[15]

The spectra in Figure 2 show that Mo and W produce different products from Cr. The major absorption at 3647.0 cm^{-1} with Mo is lower than the W counterpart at 3659.9 cm^{-1}, which is not the usual relationship for hydroxides in the same group. The M−H stretching region also contains more product absorptions for the heavier metals. In addition calculations have shown that higher oxidation state products are relatively more stable for Mo and W than for Cr; hence, we expect a different product distribution.

HMoO(OH). The new absorptions at 3690.8, 1781.5, and 712.6 cm^{-1} follow the Cr analogues. Our calculations predict these modes 5 cm^{-1} lower, 9 cm^{-1} higher, and 49 cm^{-1} lower for the Mo species, and we observed them 24 cm^{-1} lower, 29 cm^{-1} higher, and 36 cm^{-1} lower. This is acceptable agreement for these calculations using SDD pseudopotentials for each metal center. Note that the Mo reaction proceeds on 20 K annealing to increase slightly the HMoO(OH) product.

H_2MoO_2. The weaker 1861.0 and 1864.0 cm^{-1} bands are appropriate for antisymmetric and symmetric Mo−H stretching modes as predicted by our calculation for the stable hydride−oxide (Table 8). The 1337.8 cm^{-1} counterpart for the stronger mode defines a H/D = 1.3911 ratio, which is in accord for Mo. The 985.0 cm^{-1} band on the higher side of MoO_2 is appropriate for the antisymmetric Mo−O stretching mode absorption.[26]

$MoO_2(OH)_2$. The strong new 3647.0 cm^{-1} band and 3651.7 cm^{-1} partner appear to be antisymmetric and symmetric O−H stretching modes of a new dihydroxide product. The deuterium counterparts at 2688.6 and 2691.1 cm^{-1} (H/D ratio = 1.3565) are appropriate for an O−H stretching mode. This is confirmed by the appearance of new intermediate components within the above band pairs for the OH, OD product in the experiment using mixed H_2O_2 and D_2O_2. Our B3LYP calculations predict the strong mode for $MoO_2(OH)_2$ to fall 30 cm^{-1} below that for $OCr(OH)_2$ and to have strong and weak antisymmetric and symmetric O−H stretching modes separated by 3.8 cm^{-1}, which is in very good agreement with the experimental spectrum. Two associated bands at 979.3 and 732.1 cm^{-1} follow the calculated frequency trends and can also be assigned to the $MoO_2(OH)_2$ molecule, which is also observed for W (see below) and for uranium.[28] This molecule is very stable for certain heavy metals, and it appears to be even more stable for W than for Mo. Although metal tetrahydroxides are not observed here, these molecules are surely formed in reactions with two H_2O_2 molecules, as has been documented for group 4,[12] and the energized

TABLE 9: Calculated Frequencies (cm^{-1}) of H_2WO_2 at the B3LYP Level of Theory and Comparison with Experimental Results

H_2WO_2		D_2WO_2		$H_2W^{18}O_2$		Assignment
calcd	obsd	calcd	obsd	calcd	obsd	calcd
2005.6(a_1,92)	1932.4	1421.1(46)	1382.5	2005.6(93)	1932.5	1420.9(47)
1991.6(b_1,137)	1918.5	1415.9(71)	1377.6	1991.6(137)	1918.5	1415.9(71)
1033.3(a_1,60)	1010.1	1032.0(56)	1010.1	978.7(57)	956.4	976.9(50)
999.3(b_2,181)	969.2	994.2(174)	969.2	950.6(166)	918.5	944.3(158)
790.3(a_1,37)		562.2(20)		789.5(35)		561.7(20)
688.8(a_2,0)		503.1(0)		686.2(0)		499.6(0)
660.6(b_2,3)		477.1(3)		658.3(2)		475.7(3)
456.8(b_1,1)		352.5(2)		452.9(1)		347.5(2)
333.3(a_1,5)		332.8(5)		315.9(4)		315.6(4)

tetrahydroxides so formed can serve as precursors for other more stable products.

$$Cr(OH)_4 \rightarrow CrO_2(OH)_2 + H_2 \qquad \Delta E = +51 \text{ kcal/mol} \quad (5)$$

$$Mo(OH)_4 \rightarrow MoO_2(OH)_2 + H_2 \qquad \Delta E = -13 \text{ kcal/mol} \quad (6)$$

$$W(OH)_4 \rightarrow WO_2(OH)_2 + H_2 \qquad \Delta E = -36 \text{ kcal/mol} \quad (7)$$

$WO_2(OH)_2$. Our B3LYP calculation predicts the strong antisymmetric O−H stretching mode to be 19 cm^{-1} *higher* for $WO_2(OH)_2$ than for the Mo counterpart and to have a symmetric partner 3.7 cm^{-1} higher. The 3659.9 and 3664.4 cm^{-1} bands in Figure 2 are in good agreement with this prediction. These bands shifted to 2891.1 and 2701.6 cm^{-1} with D_2O_2 and gave 1.3564 isotopic frequency ratios. In addition mixed H_2O_2 and D_2O_2 reagent gave intermediate bands for the O−H and O−D stretching modes of the mixed isotopic molecule. The next important absorptions are the antisymmetric and symmetric W═O stretching modes computed at 979.1 and 1012.1 cm^{-1} (not scaled), and these are observed at 965.7 and 1003.6 cm^{-1}. These bands increase on UV irradiation and are the favored product using the $H_2 + O_2$ reagent. In the latter case Figure 4 compares spectra using $^{16}O_2$, a $^{16}O_2$, $^{16,18}O_2$, and $^{18}O_2$ mixture, and $^{18}O_2$. This strong mode shows a 16/18 isotopic frequency ratio of 1.0532, which is appropriate for the antisymmetric O═W═O stretching mode. With the $^{16,18}O_2$ isotopic molecule two new components are observed for antisymmetric and symmetric modes at 927.5 and 983.6 cm^{-1} in addition to the pure 16 and 18 isotopic bands. The intermediate 927.5 cm^{-1} band appears much lower than the median of pure 16 and 18 isotopic bands; however, the new 983.6 cm^{-1} band is found above the median of pure 16 and 18 isotopic bands. This isotopic intensity distribution is appropriate for two equivalent oxygen atoms with coupling of the symmetric and antisymmetric modes in the isotopic molecule of lower symmetry. The weaker symmetric mode at 1003.6 cm^{-1} exhibits a higher 1.0561 isotopic 16/18 frequency ratio as is appropriate.[26] Finally, three weaker lower frequency absorptions are observed at 726.3, 641.5, and 614.9 cm^{-1}, which are in very good agreement with the calculated frequencies (Table 7).

H_2WO_2. New W−O stretching modes at 969.2 and 1010.1 cm^{-1} track with two new W−H stretching modes at 1918.5 and 1932.3 cm^{-1} in laser-ablated tungsten atom reactions with H_2O_2 (Table 9). These bands were observed on deposition, increased 50% on annealing to 20 K, and increased slightly on irradiation with full-arc light. With D_2O_2 the W−O stretching mode absorption does not change, suggesting no H coupling occurs for this mode, but the W−D stretching modes shift to 1377.6 and 1382.5 cm^{-1}, respectively, giving 1.3978 and 1.3926 H/D ratios, which are typical ratios for tungsten hydrides.[1] These absorptions also increase 50% on annealing to 20 K. The same bands were observed in separate experiments with $O_2 + H_2$ and $O_2 + D_2$ as reagents. Using $^{18}O_2 + H_2$ the W═O stretching mode shifts to 918.5 cm^{-1}, giving a 1.0552 isotopic 16/18 frequency ratio, which is typical for tungsten oxide defined in our early report,[26] while the W−H stretching mode is essentially the same as those observed in H_2O_2 and $H_2 + O_2$ experiments (see Table 3).

Our DFT calculation confirms this assignment. Antisymmetrc and symmetric W−H stretching modes are predicted at 2005.6 and 1991.6 cm^{-1}, which are overestimated by 3.8%. The H/D ratios for two modes are predicted to be slightly higher (1.4113 and 1.4066) but in very good agreement with early tungsten hydride calculations.[1] The observed and calculated W−H stretching modes are higher than those of most tungsten hydrides, indicating oxygen atoms withdraw electrons from the tungsten center and very polarized W−H bonds are produced. Antisymmetric and symmetric W═O stretching modes predicted at 1033.3 and 999.3 cm^{-1} match the observed values at 1010.1 and 969.2 cm^{-1} very well.

Reaction of a tungsten atom with H_2O_2 gives the straightforward product $W(OH)_2$ first based on the weak O−O bond, although the $W(OH)_2$ intermediate is not trapped in solid argon because of its higher energy. It is energetically feasible for $W(OH)_2$ to isomerize to HWO(OH) and further to H_2WO_2 (reaction 8; Figure 6) in the laser ablation process, on annealing to 20 K to allow reagent diffusion, and on subsequent UV irradiation. The same reaction products, H_2WO_2 and HWO(OH), were observed with the $H_2 + O_2$ reagent, suggesting that W atoms react with O_2 to give WO_2 and further react with H_2. Reaction 8 is spontaneous in the 20 K argon matrix, but the analogous reaction with H_2 and O_2 requires UV irradiation.

$$W + H_2O_2 \rightarrow W(OH)_2 \rightarrow HWO(OH) \rightarrow H_2WO_2 \quad (8)$$

$HWO_2(OH)$. The sharp new even higher band at 1958.7 cm^{-1} in the W−H stretching region suggests another tungsten(VI) hydride species, and the single W−H mode appearing above those for H_2WO_2 suggests that a more electronegative substituent is also involved. Unfortunately the deuterium counterpart is masked by HOD absorption. These requirements are satisfied by the $HWO_2(OH)$ molecule, and a calculation was performed to test this hypothesis. The single W−H stretching mode was predicted to be 30 cm^{-1} higher than the upper band for H_2WO_2, and the above band is 26 cm^{-1} higher. Furthermore, the O−H stretching mode is computed between the two modes for $WO_2(OH)_2$, and a sharp new band appears in that position at 3661.9 cm^{-1}. The strong W═O mode is predicted between those for the above two molecules, and this mode is probably masked thereunder. The above evidence supports the identification of the $HWO_2(OH)$ molecule, which we expect as a byproduct of exothermic reaction 7. Thus, we have experimental and computational evidence for three related W(VI) species H_2WO_2, $HWO_2(OH)$, and $WO_2(OH)_2$ whose structures are shown in Figure 7.

TABLE 10: Calculated Frequencies (cm^{-1}) of HWO(OH) at the B3LYP Level of Theory and Comparison with Experimental Results

HWO(OH)		DWO(OD)		$HW^{18}O(^{18}OH)$		$DW^{18}O(OD)$
calcd	obsd	calcd	obsd	calcd	obsd	calcd
3908.2(a,199)	3691.1	2847.7(134)	2733.2	3895.2(192)	3680.1	2829.1(126)
1965.8(a,117)	1891.5	1395.0(60)	1355.2	1965.7(117)	1891.5	1394.9(60)
1006.4(a,159)	984.2	1005.0(153)	–	953.9(147)	935.7	952.2(140)
722.6(a,91)		674.2(141)		705.5(61)		644.0(123)
648.7(a,15)		483.3(4)		635.0(21)		480.5(4)
530.0(a,148)		416.5(59)		520.4(154)		408.7(61)
392.3(a,112)		307.6(62)		387.7(111)		301.6(61)
186.7(a,9)		175.1(10)		178.6(8)		168.5(9)
156.0(a,6)		118.4(2)		155.0(6)		117.4(2)

HWO(OH). Weak bands at 1891.5 cm^{-1} (W−H stretch), 3678.6 cm^{-1} (O−H stretch), and 984.2 cm^{-1} (W═O stretch) were observed on deposition in laser-ablated W atom reactions with H_2O_2 in excess argon (Table 10). These bands increased slightly on UV irradiation. Experiments with $H_2 + O_2$ gave the same bands, but the band contours are slightly broad because of different reagents. With D_2O_2 the W−H and O−H stretching modes shift to 1355.2 cm^{-1} (W−D stretch; H/D = 1.3957), 2712.6 cm^{-1} (O−D stretch; H/D = 1.3564), but the W═O stretching frequency is masked by D_2O_2 absorption. In the $^{18}O_2 + H_2$ experiment the W−H stretching mode shows no shift, but the stronger W═O frequency shifts 935.7 cm^{-1}, which also shows a doublet in experiment with $^{16}O_2/^{16}O^{18}O/^{18}O_2 + H_2$, suggesting that one O atom is involved in this W═O stretching mode. These bands are appropriate for the HWO(OH) molecule.

This assignment is also supported by theoretical calculations. Our B3LYP results predicted the O−H stretching mode at 3908.2 cm^{-1}, the W−H stretching mode at 1965.8 cm^{-1}, and the W═O stretching mode at 1006.4 cm^{-1}, which are overestimated by 5.9, 3.8, and 2.2%, indicating the reproduction of observed values very well. The predicted W−H stretching mode is slightly lower and the W═O mode is slightly higher than these modes in H_2WO_2, which is in good agreement with experimental observations.[11−15]

HWO_2. Two weak bands at 1906.1 cm^{-1} (W−H stretching) and 948.0 cm^{-1} (W═O stretching) track together in the W + H_2O_2 experiment, which were observed on deposition but did not change their intensities much on further annealing and irradiation. With D_2O_2 the W−H mode shifts to 1366.2 cm^{-1} but the W═O mode is essentially the same. The same bands were observed in the $H_2 + O_2$ and $D_2 + O_2$ experiments, respectively. With $H_2 + {}^{18}O_2$ the W═O stretching mode shifts to 896.3 cm^{-1}, defining the $^{16}O/^{18}O = 1.0577$ ratio, but the W−H mode shows no shift. The HWO_2 molecule is appropriate for this group of bands.

Our DFT calculation matches experimental observations very well. The W−H stretching mode of HWO_2 is predicted at 1978.6 cm^{-1}, which is overestimated by 3.8%. The W═O symmetric mode calculated at 976.2 cm^{-1} is in good agreement with the observed value, but the W═O antisymmetric mode predicted at 1017.0 cm^{-1} with weak intensity is not observed in our experiments.

HWO. Two new bands at 1790.2 cm^{-1} (W−H stretching) and 953.5 cm^{-1} (W═O stretching) were observed on deposition of W atoms with H_2O_2, which were doubled on 240−380 nm irradiation but decreased on further annealing. With D_2O_2 the W−D stretching mode was found at 1283.9 cm^{-1}, defining a 1.3943 H/D ratio, but unfortunately the W═O stretching mode is covered by a very strong D_2O_2 band centered at 952 cm^{-1}. It is interesting to note these bands were not observed with either $H_2 + O_2$ or $D_2 + O_2$, which was also the case for the monohydroxide CrOH. We propose HWO as the assignment, which is supported by DFT. The calculated W−H and W═O stretching modes are at 1858.0 and 986.6 cm^{-1}, respectively, which match observed 1790.2 and 953.5 cm^{-1} values very well. The errors are consistent with other tungsten hydroxide calculations.

Structures and Bonding. Cr and W atoms react with H_2O_2 to give strikingly different product preferences, $Cr(OH)_2$ and H_2WO_2, suggesting different product stabilities, although Cr and W are in the same transition metal group (Figure 6). This is easily understandable when we consider the outermost orbitals available for bonding. Obviously the participations of electron occupied d orbitals in bonding may be particularly important. For example valence-bonded WH_6 with orthogonal sd^5 hybrids prefers a trigonal prismatic C_{3v} structure with low electron spin state, while only the hydride complex $CrH_2(H_2)_2$ with high electron spin state is obtained for the chromium case, suggesting 3d electrons are not strongly involved in the bonding. The same reasoning applies to W and Cr reactions with H_2O_2; a W atom inserting into the O−O bond of H_2O_2 to form the hydroxide $W(OH)_2$ is the first reaction step, which is similar to most transition metal atom reactions with H_2O_2,[11−15] however strong participation of 5d electrons in σ bonding for tungsten induced H migration to W to form H_2WO_2. For chromium the hydroxide $Cr(OH)_2$ is the most stable form since the 3d orbital is corelike and less reactive. The energy difference for group 6 metal hydroxides and hydride oxides is shown in Figure 5. The $W(OH)_2$ and $Mo(OH)_2$ molecules are higher in energy than H_2WO_2 and H_2MoO_2, while $Cr(OH)_2$ is the lowest in energy. With the same reason CrOH and OCr(OH) are trapped, while HWO and HWO_2 are formed in the solid argon matrix.

Analogous Nd and U atom reactions with H_2O_2 produced $Nd(OH)_2$ and H_2UO_2, respectively (Figure 8), in which uranium favors the higher oxidation state while Nd favors the lower oxidation state.[28] As we already know the 4f orbital of the lanthanides is compacted and corelike, and only s and d electrons are involved in σ bonding. However the early 5f electrons are strongly involved in bonding.[3b] Theoretical calculations suggest UH_6 with O_h symmetry is the most stable form for uranium hexahydride, though it is not observed experimentally as the barrier for the exothermic dissociation $UH_6 \rightarrow UH_4 + H_2$ is extremely low.[29]

Both W and U favor the high oxidation state H_2MO_2 and $MO_2(OH)_2$ molecules, but the structures are slightly different. The H_2UO_2 molecule is planar with C_{2h} symmetry, while H_2WO_2 is stabilized as a nonplanar structure with C_{2v} symmetry (Figure 8). Clearly the structure of H_2WO_2 is derived from the prismatic structural preference (nonoctahedral) for WH_6, and planar H_2UO_2 inherits undoubtedly from octahedral structure. In the $MO_2(OH)_2$ case, the OUO angle is almost linear, whereas the OWO angle is nearly tetrahedral. This structural difference reflects the d and f orbital participation in bonding and polarization of the outermost core shell. As expected the 5f orbital is more expanded than the 5d orbital.[3] As a result the uranium is

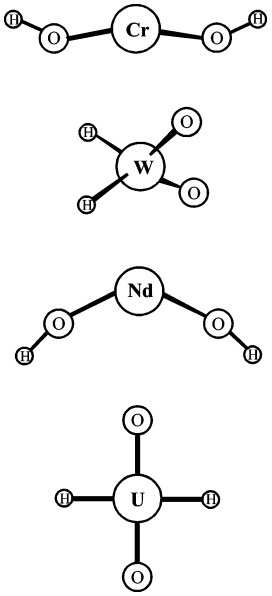

Figure 8. Structures of $Cr(OH)_2$, H_2WO_2, $Nd(OH)_2$, and H_2UO_2.

more ionic, the covalence of U−O and U−H bonds is reduced, and thereby the repulsion of ligands increases. For H_2WO_2 less tungsten ionization and less repulsion are obtained and the distorted structure is expected.

Conclusions

Cr, Mo, and W atoms react with H_2O_2 to form a variety of different hydride−hydroide−oxide products, which are trapped in solid argon for infrared spectroscopic characterization. DFT frequency, structure, and energy calculations show that higher oxidation state products are favored for the heavier Mo and W reaction products and lower oxidation state products dominate the Cr reaction chemistry. Perhaps the most interesting new molecules characterized here are $Cr(OH)_2$, H_2MoO_2, and H_2WO_2, and the series $CrO(OH)_2$, $MoO_2(OH)_2$, and $WO_2(OH)_2$. Also interesting is the increased reactivity of the cold metal atoms with H_2O_2 from Cr to Mo to W as judged by the increase in the HCrO(OH), HMoO(OH), and H_2WO_2 primary reaction product absorptions on annealing the solid argon matrix to 20 K. In all cases the higher oxidation state products require UV irradiation for an increase in the initial yield on sample deposition.

Acknowledgment. We gratefully acknowledge financial support from the National Science Foundation.

References and Notes

(1) (a) Wang, X.; Andrews, L. *J. Am. Chem. Soc.* **2002**, *124*, 5636. (b) Wang X.; Andrews, L. *J. Phys. Chem. A* **2002**, *106*, 6720. (WH_2, WH_4, and WH_6 in solid argon and neon). (c) Wang, X.; Andrews, L. *J. Phys. Chem. A* **2003**, *107*, 570. (Cr + H_2). (d) Wang, X.; Andrews, L. *J. Phys. Chem. A* **2005**, *109*, 9021. (Mo + H_2).

(2) (a) Cho, H. G.; Andrews, L. *Inorg. Chem.* **2005**, *44*, 7634. (Cr, W + CH_4). (b) Cho, H. G.; Andrews, *J. Am Chem. Soc.* **2005**, *127*, 8726. (Mo + CH_4).

(3) (a) Kaupp, M. *Angew. Chem., Int. Ed.* **2001**, *40*, 3534. (b) Straka, M.; Hrobarik, P.; Kaupp, M. *J. Am. Chem. Soc.* **2005**, *127*, 2591.

(4) (a) Shen, M.; Schaefer, H. F., III.; Partridge, H. *J. Chem. Phys.* **1993**, *98*, 508. (b) Kang, S. K.; Tang, H.; Albright, T. A. *J. Am. Chem. Soc.* **1993**, *115*, 1971. (c) Tanpipat, N.; Baker, J. *J. Phys. Chem.* **1996**, *100*, 19818. (d) Kaupp, M. *J. Am. Chem. Soc.* **1996**, *118*, 3018. (WH_6 theoretical calculations).

(5) (a) Bosworth, Y. M.; Clark, R. J. H.; Rippon, D. M. *J. Mol. Spectrosc.* **1973**, *46*, 240. (b) Claassen, H. H.; Goodman, G. L.; Holloway, J. H.; Selig, H. *J. Chem. Phys.* **1970**, *53*, 341.

(6) Jacobs, J.; Muller, H. S.; Willner, H.; Jacob, E.; Burger, H. *Inorg. Chem.* **1992**, *31*, 5357.

(7) Quinones, G. S.; Hagele, G.; Seppelt, K. *Chem. Eur. J.* **2004**, *L10*, 4755.

(8) Vanquickenborne, L. G.; Vinckier, A. E.; Pierloot, K. *Inorg. Chem.* **1996**, *35*, 1305.

(9) Russo, T. V.; Marstin, R. L.; Hay, P. J. *J. Chem. Phys.* **1995**, *102*, 8023.

(10) Marsden, C. J.; Moncrieff, D. Quelch. G. E. *J. Phys. Chem.* **1994**, *98*, 2038.

(11) Wang, X.; Andrews, L. *J. Phys. Chem. A* **2005**, *109*, 3849. (Zn, Cd, Hg + H_2O_2).

(12) (a) Wang, X.; Andrews, L. *Inorg. Chem.* **2005**, *44*, 7189. (b) Wang, X.; Andrews, L. *J. Phys. Chem. A* **2005**, *109*, 10689. (Group 4 + H_2O_2).

(13) Wang, X.; Andrews, L. *Inorg. Chem.* **2005**, *44*, 9076. (Cu, Ag, Au + H_2O_2).

(14) (a) Wang, X.; Andrews, L. *J. Phys. Chem. A* **2006**, *110*, 1850. (Sc + H_2O_2). (b) Wang, X.; Andrews, L. *J. Phys. Chem. A* **2006**, *110*, 4157. (Y, La + H_2O_2).

(15) Wang, X.; Andrews, L. *J. Phys. Chem. A*, in press. (Mn, Fe, Co, Ni + H_2O_2).

(16) Andrews, L. *Chem. Soc. Rev.* **2004**, *33*, 123.

(17) Andrews, L.; Citra. A. *Chem. Rev.* **2002**, *102*, 885.

(18) Pettersson, M.; Tuominen, S.; Rasanen, M. *J. Phys. Chem. A* **1997**, *101*, 1166.

(19) Pehkonen, S.; Pettersson, M.; Lundell, J.; Khriachtchev, L.; Rasanen, M. *J. Phys. Chem. A* **1998**, *102*, 7643.

(20) Frisch, M. J.; Trucks, G. W.; Schlegel, H. B.; Scuseria, G. E.; Robb, M. A.; Cheeseman, J. R.; Zakrzewski, V. G.; Montgomery, J. A., Jr.; Stratmann, R. E.; Burant, J. C.; Dapprich, S.; Millam, J. M.; Daniels, A. D.; Kudin, K. N.; Strain, M. C.; Farkas, O.; Tomasi, J.; Barone, V.; Cossi, M.; Cammi, R.; Mennucci, B.; Pomelli, C.; Adamo, C.; Clifford, S.; Ochterski, J.; Petersson, G. A.; Ayala, P. Y.; Cui, Q.; Morokuma, K.; Malick, D. K.; Rabuck, A. D.; Raghavachari, K.; Foresman, J. B.; Cioslowski, J.; Ortiz, J. V.; Stefanov, B. B.; Liu, G.; Liashenko, A.; Piskorz, P.; Komaromi, I.; Gomperts, R.; Martin, R. L.; Fox, D. J.; Keith, T.; Al-Laham, M. A.; Peng, C. Y.; Nanayakkara, A.; Gonzalez, C.; Challacombe, M.; Gill, P. M. W.; Johnson, B.; Chen, W.; Wong, M. W.; Andres, J. L.; Gonzalez, C.; Head-Gordon, M.; Replogle, E. S.; Pople, J. A. *Gaussian 98*, Revision A.6; Gaussian: Pittsburgh, PA, 1998.

(21) Wang, X.; Andrews, L. *J. Phys. Chem. A* **2001**, *105*, 5812.

(22) Zhou, M.; Hacalogu, J.; Andrews, L. *J. Chem. Phys.* **1999**, *110*, 9450.

(23) Milligan, D. E.; Jacox, M. E. *J. Mol. Spectrosc.* **1973**, *46*, 460.

(24) Jacox, M. E.; Thompson, W. E. *J. Chem. Phys.* **1994**, *100*, 750.

(25) Chertihin, G. V.; Bare, W. D.; Andrews, L. *J. Chem. Phys.* **1997**, *107*, 2798.

(26) (a) Bare, W. D.; Souter, P. F.; Andrews, L. *J. Phys. Chem. A* **1998**, *102*, 8279. (b) Zhou, M.; Andrews, L. *J. Chem. Phys.* **1999**, *111*, 4230.

(27) Zhou, M.; Zhang, L.; Shao, L.; Wang. W.; Fan, K.; Qin, Q. *J. Phys. Chem. A* **2001**, *105*, 10747.

(28) Wang, X.; Andrews, L. Unpublished results for Nd, 2006. (b) Wang, X.; Andrews, L.; Li, J. *Inorg. Chem.* **2006**, *45*, 4157. (c) Liang, B.; Hunt, R. D.; Kushto, G. P.; Andrews, L. *Inorg. Chem.* **2005**, *44*, 2159.

(29) Straka, M.; Hrobarik, P.; Kaupp, M. *J. Am. Chem. Soc.* **2005**, *127*, 2591.

(30) Straka, M.; Patzschke, M.; Pyykko, P. *Theor. Chem. Acc.* **2003**, *109*, 332.